Thermodynamics of the Hydration Shell. 2. Excess Volume and Compressibility of a Hydrophobic Solute

Nobuyuki Matubayasi and Ronald M. Levy*

Department of Chemistry, Rutgers University, New Brunswick, New Jersey 08903

Received: June 13, 1995; In Final Form: August 10, 1995[⊗]

The hydration shell model for the excess volume and compressibility is examined. A modified Kirkwood−Buff formula for the excess volume, which is appropriate for use in the canonical ensemble, is presented. Its pressure derivative is shown to be the excess compressibility, which can be expressed as an integral of the local solvent compressibility over the hydration shell. For methane in water, which is chosen as the first application, the local solvent density and compressibility around the solute are calculated from a Monte Carlo simulation as continuous functions of the distance from the solute. The localization of the excess volume and compressibility within the hydration shell is then analyzed in terms of the deviation of the local solvent density and compressibility from their bulk values, respectively. The effect of the exclusion of solvent molecules by the solute is also described for the excess volume. About 80% of the total excess volume is accounted for by the excluded volume effect of the solute plus the deviation of the volume per water molecule in the first hydration shell from that in the bulk, whereas the hydration shell model is not even qualitatively successful for describing the excess compressibility. A condition for the qualitative validity of the hydration shell model is identified. This involves the phase relationship between the local excess quantity and the solute−solvent radial distribution function. On the basis of an analysis of the pressure dependence of the chemical potential, the excess compressibility of the model methane−water solution is found to have a positive sign. This apparent "softness" of the "hydrophobic water", however, is not simply related to the properties of the first hydration shell.

1. Introduction

The analysis of hydration phenomena in terms of a discrete hydration shell has a long tradition. The hydration shell model accounts for excess thermodynamic quantities by attributing solvation properties to a perturbed solvent layer at the surface of the solute. In a previous paper,[1] we discussed the statistical mechanical foundation and the practical application of the hydration shell model for the excess energy of solvation. This quantity corresponds to the first derivative of the chemical potential with respect to temperature. The effect of a pressure variation on the solution process is determined by the excess volume and compressibility of solvation. The first pressure derivative of the chemical potential, the excess volume, probes the variation in the solvent density around the solute. The second pressure derivative of the chemical potential, the excess compressibility, probes the rigidity of the solvent around the solute. In this paper, we describe how the hydration shell model can be used to evaluate the excess volume and compressibility within the context of well-defined statistical mechanical procedures, and we discuss the accuracy of the hydration shell model for determining these excess thermodynamic quantities from simulations. We use methane as a model solute.

As shown by Kirkwood and Buff,[2] the excess volume is expressed in terms of the solute−solvent radial distribution function, which describes the variation in the local density of the solvent around the solute. The deviation of the local solvent density from the bulk value is integrated over the whole system to give the excess volume in the Kirkwood−Buff formula.[2] In this work, we derive a version of the Kirkwood−Buff formula for the excess volume by a different path from the one used by Kirkwood and Buff,[2] so that the local nature of the formula is more apparent. In our derivation of the excess volume formula, we employ the canonical ensemble, whereas Kirkwood and Buff based their derivation on the grand canonical ensemble. The distinction between the formulas is important because we wish to use the results of simulations in the canonical ensemble to evaluate the excess volume. As the integrand in the Kirkwood−Buff integral formula is local, it is possible to restrict the range of integration to a region proximate to the solute. Pratt and Pohorille[3] and Paulaitis *et al.*[4] have used the Kirkwood−Buff formula with a finite cutoff to evaluate the excess volume of solvation based on simulations in the canonical ensemble. The use of the Kirkwood−Buff formula in the canonical ensemble, however, requires a careful analysis of asymptotic properties of the solute−solvent radial distribution function, as we discuss in section 2. The introduction of a finite cutoff can be easily related to the hydration shell idea. Using a Kirkwood−Buff type formula, we perform a shell decomposition of the excess volume and analyze the contribution of each shell by calculating the fraction of the excess volume contained within that shell. By this procedure, we can clearly distinguish three contributions to the excess volume: (1) the volume excluded to solvent molecules by the solute, (2) the volume change due to the rearrangement of the solvent in the first solvation shell, and (3) the remaining volume change due to the rearrangement of more distant solvent molecules.

As the excess volume in the Kirkwood−Buff formula is expressed in terms of the solute−solvent radial distribution function, the excess compressibility can be expressed in terms of the pressure derivative of the radial distribution function. In section 2, we introduce a quantity called the local compressibility, which governs the response of the local density to pressure variation. The difference between the local and bulk compressibilities can be integrated over the whole system to give the excess compressibility. The concept of the hydration shell is again implemented by introducing a finite cutoff in the

[⊗] Abstract published in *Advance ACS Abstracts,* October 1, 1995.

0022-3654/96/20100-2681$12.00/0

integration. The localization of the excess compressibility can then be analyzed by calculating the fraction contained within the hydration shell as a function of the shell cutoff radius. The hydration shell analysis of the excess volume and compressibility is parallel to that of the excess energy described in the previous paper.[1]

In section 2, we express the excess volume and compressibility in terms of the solute−solvent radial distribution function and its pressure derivative and show how the hydration shell concept is introduced for these excess thermodynamic quantities. Section 3 presents the simulation technique, and the results are given and discussed in section 4. There the radial distribution function and its pressure dependence are examined, and their connection to the calculations of the excess volume and compressibility is discussed.

2. Theory

In this section, we describe how the hydration shell concept is introduced into the statistical mechanical formulas for the excess volume and compressibility. The solute−solvent radial distribution function plays an important role in these excess quantities. The formulation given below is independent of the choice of the potential functions and is applicable not only to the example of methane in water treated in this paper but also to any solute and solvent.

2.1. Excess Volume. Consider the process of solute insertion at constant volume. We adopt periodic boundary conditions as implemented in computer simulations. Let N and V be respectively the number of solvent molecules in the unit cell and the volume of the unit cell. As the pure solvent is homogeneous or translationally invariant due to the periodic boundary condition, the density of the pure solvent system is independent of the position and equal to $\rho_0 \stackrel{\text{def}}{=} N/V$. Let the solute be inserted at the (arbitrarily chosen) fixed origin. The solute−solvent distribution function, $\rho(\vec{r})$, is then a function of the position of the solvent molecule, $\vec{r}$. Since the solute is fixed at the origin, $\rho(\vec{r})$ is actually $\rho_0 g_{uv}(\vec{r})$, where $g_{uv}(\vec{r})$ is the solute−solvent radial distribution function. When the solute−solvent interaction is viewed as an external field for the solvent molecules, $\rho(\vec{r})$ can be considered the one-particle distribution function of the solvent at the point $\vec{r}$. The asymptotic value of $g_{uv}(\vec{r})$ plays an important role in molecular expressions for excess thermodynamic quantities. For the constant volume process of solute insertion considered here, it was shown in Appendix 1 of the previous paper[1] that when $|\vec{r}|$ is much larger than the solute−solvent correlation length,

$$\rho(\vec{r}) \to \varrho_0 - \Delta V \frac{\partial \rho_0}{\partial V} + o\left(\frac{1}{V}\right) = \frac{N}{V - \Delta V} + o\left(\frac{1}{V}\right) \tag{2.1}$$

where ΔV is the excess volume of solution in the constant-pressure process with the pressure determined by the number density ρ_0 through the equation of state and $o(1/V)$ denotes a variable which vanishes faster than $1/V$ in the thermodynamic limit ($V \to \infty$). It should be noted that as the solute is fixed at the origin, ΔV is the pressure derivative of the pseudo chemical potential in the notation of Ben-Naim[5] and its ideal contribution is excluded from the outset. In other words,

$$\Delta V = \overline{V_s} - kT\kappa_0 \tag{2.2}$$

where $\overline{V_s}$ is the partial molar volume of the solute at infinite dilution, k is the Boltzmann constant, T is the temperature, and κ_0 is the isothermal compressibility of the pure solvent. Let $\rho(\infty)$ be the asymptotic value of $\rho(\vec{r})$, $N/(V - \Delta V)$, as given in eq 2.1. Using the fact that the volume integral of $\rho(\vec{r})$ is equal to N, it is easy to show

$$\Delta V = -\int_V d\vec{r} \left(\frac{\rho(\vec{r})}{\rho(\infty)} - 1\right) + o(1) = \int_V d\vec{r}\ \rho(\vec{r})\left(\frac{1}{\rho(\vec{r})} - \frac{1}{\rho(\infty)}\right) + o(1) \tag{2.3}$$

where $o(1)$ denotes a variable which vanishes in the thermodynamic limit. Since $1/\rho_0$ is the volume per solvent molecule in the bulk, by analogy $1/\rho(\vec{r})$ can be interpreted as the volume per solvent molecule at the position $\vec{r}$ in the solution. Equation 2.3 shows that the deviation of the local solvent volume per molecule from its limiting value is summed up over all the solvent molecules in the system to give the total excess volume. Note the similarity of eq 2.3 to the Kirkwood−Buff formula of the excess volume,[2,5]

$$\Delta V = -\int_V d\vec{r}\ (g_{uv}(\vec{r}) - 1) + o(1) \tag{2.4}$$

which is derived for the grand canonical ensemble rather than for the canonical ensemble considered in this work. The difference between eq 2.3 for ΔV in the canonical ensemble and the Kirkwood−Buff formula for ΔV in the grand canonical ensemble is due to the difference in the asymptotic values of $g_{uv}(\vec{r})$ in these two ensembles. However, the two expressions for ΔV are identical when a finite cutoff is introduced into the integrals, as discussed below.

The introduction of a cutoff at the distance λ from the solute is equivalent to the assumption that the solvent density reaches its asymptotic value at $|\vec{r}| = \lambda$. When this condition is valid and a finite cutoff is used, $\rho(\infty)$ can be replaced by ρ_0 in eq 2.3 in the thermodynamic limit (neglect of $o(1)$ terms). The expression for the excess volume can then be written as

$$\Delta V = \int_{|\vec{r}|<\lambda} d\vec{r}\ \rho(\vec{r})\left(\frac{1}{\rho(\vec{r})} - \frac{1}{\rho_0}\right) = -\int_{|\vec{r}|<\lambda} d\vec{r}\ (g_{uv}(\vec{r}) - 1) \stackrel{\text{def}}{=} \Delta V(\lambda) \tag{2.5}$$

Equation 2.5 is a local expression and is thus independent of the ensemble. It corresponds to the Kirkwood−Buff formula with a finite cutoff. Note that our derivation of ΔV in the canonical ensemble is different from that of Kirkwood and Buff in the grand canonical ensemble.

In any practical implementation by computer simulations, the Kirkwood−Buff formula is applied with a finite cutoff. But the validity of this is based on the fact that the asymptotic value of $g_{uv}(\vec{r})$ differs from 1 by order $o(1/V)$ in the grand canonical ensemble. However, the asymptotic behavior of $g_{uv}(\vec{r})$ in the grand canonical ensemble is different from that of $g_{uv}(\vec{r})$ in the canonical ensemble. Thus, in the canonical ensemble, where most simulations are performed, a finite volume correction to eq 2.5 is needed when a large cutoff λ is used. As a striking example, if λ is large enough to include the whole simulation box, i.e., if a cutoff is not applied to the integral in eq 2.5, $\Delta V(\lambda)$ calculated by eq 2.5 is simply zero due to the conservation of the number of particles. Such a procedure is, of course, incorrect because eq 2.3 has to be used in the canonical ensemble if too large a cutoff is applied rather than the Kirkwood−Buff formula given in eq 2.4.

When the solute molecule and the solvent water molecule cannot come closer than a distance σ (i.e., for a hard-sphere solute), eq 2.5 can be rewritten:

$$\Delta V(\lambda) = V_0 + N(\lambda)\left(\bar{v}(\lambda) - \frac{1}{\rho_0}\right) \tag{2.6}$$

where

$$V_0 = \frac{4}{3}\pi\sigma^3 \tag{2.7}$$

$$N(\lambda) = \int_{|\vec{r}|<\lambda} \mathrm{d}\vec{r}\ \rho(\vec{r}) \tag{2.8}$$

and

$$\bar{v}(\lambda) = \frac{\int_{\sigma<|\vec{r}|<\lambda} \mathrm{d}\vec{r}}{\int_{\sigma<|\vec{r}|<\lambda} \mathrm{d}\vec{r}\ \rho(\vec{r})} \tag{2.9}$$

In this equation, V_0 is the volume excluded from solvent molecules by the solute, $N(\lambda)$ is the number of water molecules in the hydration shell $|\vec{r}| < \lambda$, and $\bar{v}(\lambda)$ is the average volume occupied by a water molecule in the hydration shell. As the excluded volume is the excess volume in the low-density limit, where the solvent−solvent correlation is absent,[6] the first term in eq 2.6 can be considered an ideal or "intrinsic" contribution to the excess volume, and the second term describes the nonideal effect of the solvent reorganization in the hydration shell due to the presence of the solute. Historically, the concept of the intrinsic volume was first formulated to be the van der Waals volume of the solute by Evans and Polanyi,[7] but it was pointed out by Yoshimura *et al.*[6,8] and Ladanyi and Hynes[9] that such a formulation does not provide a clear account of experimental results. Within the statistical mechanical framework provided by eqs 2.3, 2.5, and 2.6, it is natural to define the intrinsic volume as the volume excluded from the solvent by the solute, rather than as the van der Waals volume of the solute. With this definition, the intrinsic volume is just the volume corresponding to the region where $g_{\mathrm{uv}}(\vec{r})$ is zero. The excluded volume is experimentally accessible through measurements of the second virial coefficients,[6] while the van der Waals volume is not. It is also shown in section 4.4 that the van der Waals volume of the solute is not a good choice for the intrinsic volume from the perspective of the hydration shell decomposition. For simplicity, we hereafter call the first term of eq 2.6 the excluded volume and the second term the hydration volume.

The statistical mechanical formulas for the excess volume in this section apply to a solute of any shape or interaction. For a realistic solute−solvent interaction potential, there arises an ambiguity in the definition of the excluded volume because of the softness of the solute−solvent interaction. This ambiguity is less significant for large solutes such as proteins. In a forthcoming paper, we will use eq 2.6 as the basis for analyzing volume changes associated with protein folding.[10]

2.2. Excess Compressibility. The excess compressibility governs the response of the excess volume to pressure variation. We define the excess compressibility, $\Delta\kappa$, as

$$\Delta\kappa = -\rho_0 \frac{\partial \Delta V}{\partial P} \tag{2.10}$$

where ρ_0 and P are respectively the density and the pressure of the pure solvent. The factor ρ_0 makes $\Delta\kappa$ as defined above have units of reciprocal pressure, which is the common unit for compressibilities. Due to the minus sign in eq 2.10, $\Delta\kappa$ is positive when the solution is more compressible than the pure solvent, and it is negative when the solution is less compressible. The factor $-\rho_0$ also simplifies the hydration shell formula for the excess compressibility derived below.

In order to express the excess compressibility as an integral over local quantities, we begin with eq 2.3. Since $\rho(\vec{r})$ at distances far from the solute differs from $\rho(\infty)$ by order $o(1/V)$, the definition in eq 2.10 gives

$$\begin{aligned}\Delta\kappa &= \rho_0 \int_V \mathrm{d}\vec{r}\ \frac{\partial}{\partial P}\left(\frac{\rho(\vec{r})}{\rho(\infty)}\right) + o(1) \\ &= \rho_0 \int_V \mathrm{d}\vec{r}\ \frac{\rho(\vec{r})}{\rho(\infty)} \frac{\partial}{\partial P}\left(\ln \frac{\rho(\vec{r})}{\rho(\infty)}\right) + o(1) \\ &= \int_V \mathrm{d}\vec{r}\ \rho(\vec{r})\left(\frac{\partial \ln(\rho(\vec{r}))}{\partial P} - \frac{\partial \ln(\rho(\infty))}{\partial P}\right) + o(1)\end{aligned} \tag{2.11}$$

In the last line of this equation, the property is used that $\rho(\infty)$ differs from ρ_0 by order $o(1)$. Since $\partial \ln \rho_0/\partial P$ is the compressibility of the pure solvent (bulk compressibility) κ_0, by analogy $\partial \ln(\rho(\vec{r}))/\partial P$ can be interpreted as the local compressibility of the solvent at $\vec{r}$ in the solution. It is the rate of change in the density of the solvent at $\vec{r}$ with pressure variation. Equation 2.11 shows that the deviation of the local solvent compressibility from its limiting value is summed up over all the solvent molecules in the system to give the total excess compressibility.

The concept of the hydration shell is implemented by introducing a cutoff in the integral in eq 2.11. The introduction of a cutoff at the distance λ from the solute is equivalent to the assumption that the local solvent compressibility reaches its asymptotic value at $|\vec{r}| = \lambda$. When this condition is valid,

$$\begin{aligned}\Delta\kappa &= \int_{|\vec{r}|<\lambda} \mathrm{d}\vec{r}\ \rho(\vec{r})\left(\frac{\partial \ln(\rho(\vec{r}))}{\partial P} - \frac{\partial \ln \rho_0}{\partial P}\right) \\ &= \int_{|\vec{r}|<\lambda} \mathrm{d}\vec{r}\ \rho(\vec{r}) \frac{\partial \ln(g_{\mathrm{uv}}(\vec{r}))}{\partial P} \\ &= \rho_0 \int_{|\vec{r}|<\lambda} \mathrm{d}\vec{r}\ \frac{\partial g_{\mathrm{uv}}(\vec{r})}{\partial P} \overset{\mathrm{def}}{=} \Delta\kappa(\lambda)\end{aligned} \tag{2.12}$$

in the thermodynamic limit (neglect of $o(1)$ terms). Note that when λ is fixed at a finite value, $\partial \ln \rho(\infty)/\partial P$ can be replaced by $\partial \ln \rho_0/\partial P$ in the thermodynamic limit. Equation 2.12 is a local expression and is thus independent of the ensemble. This hydration shell formula with the cutoff λ can also be expressed in a convenient manner:

$$\Delta\kappa(\lambda) = N(\lambda)(\bar{\kappa}(\lambda) - \kappa_0) \tag{2.13}$$

where

$$N(\lambda) = \int_{|\vec{r}|<\lambda} \mathrm{d}\vec{r}\ \rho(\vec{r}) \tag{2.14}$$

and

$$\bar{\kappa}(\lambda) = \frac{\int_{|\vec{r}|<\lambda} \mathrm{d}\vec{r}\ \rho(\vec{r})(\partial \ln(\rho(\vec{r}))/\partial P)}{\int_{|\vec{r}|<\lambda} \mathrm{d}\vec{r}\ \rho(\vec{r})} = \frac{\partial \ln N(\lambda)}{\partial P} \tag{2.15}$$

In other words, $N(\lambda)$ is the number of solvent molecules within the hydration shell $|\vec{r}| < \lambda$ and $\bar{\kappa}(\lambda)$ is the average local compressibility of the solvent within $|\vec{r}| < \lambda$. The latter is also the rate of change in the number of solvent molecules in the shell or the rate of change in the solvent density in the shell. Equation 2.13 shows that the introduction of the hydration shell concept with any λ makes it possible to express the excess compressibility by only two quantities, the average local compressibility (shell compressibility) and the bulk compressibility.

3. Simulation Procedures

In order to calculate $g_{uv}(\vec{r})$, Monte Carlo statistical mechanical simulations[11] were carried out in the canonical ensemble at a temperature of 10 °C and solvent densities of 1.0 and 1.1 g/cm^3. In these simulations, 647 water molecules and 1 methane molecule were located in cubic cells with edge lengths of 26.9 and 26.0 Å, respectively. The water molecule was modeled with the TIP4P potential,[12] and the water−methane interaction was taken to be the Lennard-Jones 12−6 type with $\sigma_{MO} = 3.45$ Å and $\epsilon_{MO} = 0.21$ kcal/mol.[13] All the interactions were spherically truncated at 8.5 Å. Periodic boundary conditions in the minimum image convention were employed. To enhance the statistics for the solute and its neighboring water molecules, preferential sampling was used.[11,14] The simulation was performed for 2000K passes at each density (1 pass consists of 648 attempted moves). The density dependence of $g_{uv}(\vec{r})$ is converted to the pressure dependence by

$$\frac{\partial g_{uv}(\vec{r})}{\partial P} = \varrho_0\kappa_0 \frac{\partial g_{uv}(\vec{r})}{\partial \varrho_0} \tag{3.1}$$

where P, ϱ_0, and κ_0 are respectively the pressure, the density, and the isothermal compressibility of the pure solvent. The procedure for calculating κ_0 for the pure solvent is described below.

To evaluate the errors in the excess volume and compressibility introduced by employing a shell cutoff, the "exact" values independent of the cutoff are required for the excess volume and compressibility of the system under investigation (TIP4P water + LJ methane). The excess volume ΔV and the excess compressibility $\Delta\kappa$ of the methane in water solution can be determined from the pressure dependence, or equivalently, the density dependence of the chemical potential through second order. In order to calculate the "exact" values, we make use of the equations

$$\Delta V = \frac{\partial \Delta\mu}{\partial P} = \varrho_0\kappa_0 \frac{\partial \Delta\mu}{\partial \varrho_0} \tag{3.2}$$

$$\Delta\kappa = -\varrho_0 \frac{\partial \Delta V}{\partial P} = -\left(\kappa_0 + \frac{\partial \ln \kappa_0}{\partial P}\right)(\varrho_0 \Delta V) - \varrho_0(\varrho_0\kappa_0)^2 \frac{\partial^2 \Delta\mu}{\partial \varrho_0^{\,2}} \tag{3.3}$$

where $\Delta\mu$ is the chemical potential of the solute inserted at a fixed point.

To calculate $\Delta\mu$ as a function of the solvent density, Monte Carlo simulations were carried out in the canonical ensemble at a temperature of 10 °C and densities of 0.985, 1.000, and 1.015 g/cm^3. In these simulations, 647 water molecules were located in the unit cell. The interaction potential and the boundary conditions were the same as those for the solution of methane in water. A methane molecule was treated as a test particle, and the particle insertion method[1,15] was employed to calculate the chemical potential at each density. The simulation was performed for 800K passes at each density. The chemical potentials calculated at the densities listed above were used to evaluate the first and second density derivatives of the chemical potential at the solvent density of 1 g/cm^3 by finite difference.

To evaluate κ_0, the volume fluctuations of the pure solvent were calculated through Monte Carlo simulations in the NPT (isobaric−isothermal) ensemble at a temperature of 10 °C and pressures of 1.0 and 1000 atm. In these simulations, 647 water molecules were located in the unit cell, and the interaction potential and the boundary conditions were the same as those for the solution of methane in water. The simulation was performed for 500K passes at each pressure.

In applying eqs 3.2 and 3.3 to evaluate ΔV and $\Delta\kappa$, we examined the density dependence of the chemical potential rather than the pressure dependence of the chemical potential. This is because the particle insertion method converges much faster in the NVT (canonical) ensemble than in the NPT ensemble. We did not employ direct calculations of ΔV and $\Delta\kappa$ from the particle insertion method in the NPT ensemble, since they are even slower to converge than the calculation of the chemical potential in the NPT ensemble. The excess volume and compressibility calculated from the particle insertion method and the solvent compressibility through eqs 3.2 and 3.3 are independent of the hydration shell cutoff and are considered to be the "exact" values for the model employed.

4. Results and Discussion

4.1. Exact Results. By the particle insertion method, the chemical potentials $\Delta\mu$ were calculated to be 2.43 ± 0.04, 2.74 ± 0.02, and 2.94 ± 0.01 kcal/mol at solvent densities of 0.985, 1.000, and 1.015 g/cm^3, respectively. This set of data was fitted to a quadratic curve to evaluate the first and second density derivatives of the chemical potential at 1.000 g/cm^3. The compressibilities of the pure solvent κ_0 were calculated from the NPT simulations to be (5.00 ± 0.06) × 10^{-5} and (3.64 ± 0.20) × 10^{-5} atm^{-1} at solvent pressures of 1.0 and 1000 atm, respectively. These are in good agreement with the experimental values, 4.8 × 10^{-5} and 3.4 × 10^{-5} atm^{-1}, respectively.[16] Our calculated compressibility κ_0 for TIP4P water is in fact in better agreement with experiment than the corresponding value originally reported by Jorgensen *et al.*,[12] although the estimated error was not reported.

Using the data above and eqs 3.2 and 3.3, the excess volume of solvation ΔV at a solvent density of 1 g/cm^3 is found to be 58.3 ± 6.5 Å^3 (35.1 ± 3.9 cm^3/mol). This value is in good agreement with the experimental value at 25 °C, 60.1 Å^3 (36.2 cm^3/mol).[5] The excess compressibility of solvation $\Delta\kappa$ at a solvent density of 1 g/cm^3 is calculated to be (3.3 ± 2.6) × 10^{-3} atm^{-1}. For example, the dissolution of 1 mol/L of methane is predicted to result in an increase of the solution compressibility by (5.8 ± 4.7) × 10^{-5} atm^{-1} (for a derivation, see the Appendix). According to this analysis for our model potential parameters, the methane−water solution is more compressible than pure TIP4P water. This behavior is not consistent with one experimental observation[17,18] that the excess compressibility per methylene group is negative,[19] while it is consistent with another experimental observation[17] that the excess compressibilities for aromatic solutes are positive (however, aromatics

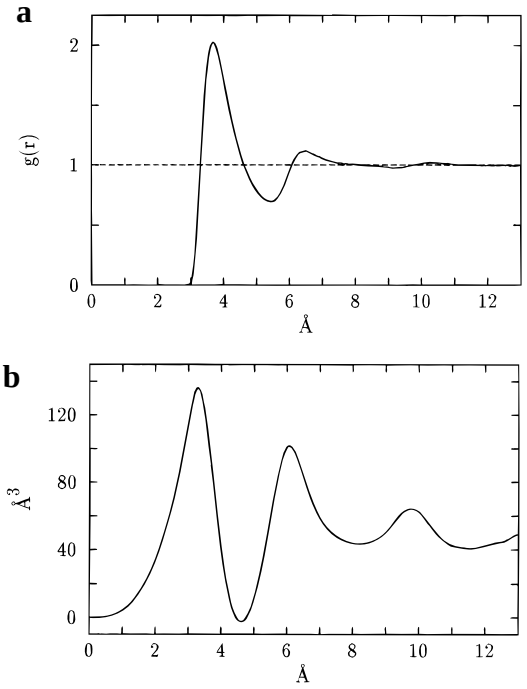

Figure 1. (a) Methane−water radial distribution function. (b) Excess volume as a function of the cutoff radius of the shell. The horizontal axis shows the cutoff radius of the shell, and the vertical axis shows the excess volume evaluated with this cutoff.

are sometimes treated as a distinct class).[20] In this connection, it is also of interest to note that the positive excess compressibility change observed upon protein unfolding has been attributed to solvent exposure of buried hydrophobic groups.[22,23] Thus, further investigation of the real and model systems is warranted for the analysis of higher order volumetric properties of aqueous solutions. We emphasize, however, that the statistical mechanical formulation and the scheme of analysis described in this paper are independent of the choice of potential functions or the solute and that the hydration shell analysis of the excess compressibility demonstrated below is internally consistent for the model employed in this work.

4.2. Excess Volume. In Figure 1, we show the methane−water radial distribution function $g_{uv}(\vec{r})$ at a solvent density of 1 g/cm^3 as a function of the distance $|\vec{r}|$ from the solute, and the excess volume of solvation $\Delta V(\lambda)$ as a function of the hydration shell cutoff radius λ. As seen from eqs 2.3 and 2.5, regions of $\vec{r}$ in which water is denser than in the bulk make a negative contribution to ΔV and regions which are less dense make a positive contribution. This feature is clearly shown in the behavior of $\Delta V(\lambda)$ in Figure 1b. The overall behavior of $\Delta V(\lambda)$ as a function of λ is similar to the results characterized by Pratt and Pohorille[3] and Paulaitis *et al.*[4] The total excess volume ΔV is smaller than the excluded volume, because of the presence of solute−solvent correlations in the vicinity of the solute. We consider below in more detail the contributions of the excluded volume and the first and outer hydration shells to the total excess volume ΔV.

The first contribution to the excess volume comes from the exclusion by the solute of the space available to the centers of the solvent molecules. But the softness of the solute−solvent interaction prevents unambiguous determination of the exclusion radius σ. In fact, $g_{uv}(\vec{r})$ in Figure 1a is not exactly zero even in the region of $|\vec{r}| < 3$ Å. In order to make a rational choice for the exclusion radius σ, we refer to the behavior of $g_{uv}(\vec{r})$ for a hard-sphere solute.

When the solute is a hard sphere with exclusion radius σ, $g_{uv}(\vec{r})$ is exactly zero for $|\vec{r}| < \sigma$ and is maximum at the contact point $|\vec{r}| = \sigma$. The contact point has two characteristics; it is the first maximum of $g_{uv}(\vec{r})$ as well as the first maximum of $\Delta V(\lambda)$. By analogy, the exclusion radius for a soft solute−solvent interaction might be taken to be the position of either the first maximum of $g_{uv}(\vec{r})$ or the first maximum of $\Delta V(\lambda)$, which corresponds to the point at which $g_{uv}(\vec{r})$ first reaches 1. However, these two values for the exclusion radius are in general not coincident for a soft solute−solvent interaction. For the model employed in this work, it is seen from Figure 1 that $g_{uv}(\vec{r})$ reaches the first maximum at $|\vec{r}| = 3.7$ Å, while $\Delta V(\lambda)$ reaches the first maximum at $\lambda = 3.3$ Å. The exclusion radius σ is thus determined to be either 3.7 or 3.3 Å. Accordingly, the excluded volume is either 90 or 136 Å^3. As both values are larger than the "exact" value for the excess volume of methane in TIP4P water determined in section 4.1, the hydration volume (the second term of eq 2.6) must be negative. In other words, the hydrating waters, whose positions are correlated with that of the solute, are, on average, denser than bulk water. As discussed in section 4.4, the choice of the exclusion radius σ determined by the first maximum of $\Delta V(\lambda)$ is superior from the perspective of the hydration shell model. Thus, from the first maximum of $\Delta V(\lambda)$ in Figure 1b, the excluded volume is found to be $V_0 = 136$ Å^3, and $\Delta V(\lambda) - V_0$ is hereafter called the hydration volume. It should be noted that the exclusion radius chosen in this way corresponds to the sum of the van der Waals radii of methane and water, $\sigma = 3.3$ Å.

The second contribution to the excess volume, the hydration volume, probes the local density of the solvent around the solute. Equation 2.5 shows that the local excess quantity for the excess volume is $1/\varrho(\vec{r}) - 1/\varrho_0$. This is proportional to $1/g_{uv}(\vec{r}) - 1$, and its variation as a function of $\vec{r}$ can be easily seen from Figure 1a. Reflecting the oscillatory nature of $1/g_{uv}(\vec{r}) - 1$, the hydration volume shows oscillatory behavior, as seen in Figure 1b. There is a negative contribution from the water molecules in the first hydration shell, and the hydration volume remains negative even when the oscillatory contributions of the outer shell water molecules are added. In simplest terms, the solvent contribution reduces the excess volume below that of the excluded volume for any cutoff. In other words, the sign of the hydration effect on the excess volume can be correctly accounted for by any cutoff. This is related to the fact that the local excess quantity $1/\varrho(\vec{r}) - 1/\varrho_0$ varies in phase with $g_{uv}(\vec{r})$. In section 4.4, we discuss how the validity of the hydration shell model depends on the phase relationship between the local excess quantity and the solute−solvent radial distribution function.

The total excess volume is determined by the balance between the exclusion effect (the first term of eq 2.6) and the hydration effect (the second term of eq 2.6). Figure 1b shows that the effect of the variation in the solvent density around methane, for which the total contribution is negative, does not converge monotonically as a function of the shell cutoff. The effect of the increased solvent density in the first peak is so large that at $\lambda \approx 4.5$ Å it almost completely cancels the positive contribution of the excluded volume and $\Delta V(\lambda) \approx 0$. The total contribution of the first shell, not that at the first maximum only, needs to be taken into account for the determination of ΔV. The oscillation of $\Delta V(\lambda)$ is damped when the shell cutoff extends beyond the first shell ($\lambda \approx 5.5$ Å). The oscillation of $g_{uv}(\vec{r})$ beyond the first shell affects $\Delta V(\lambda)$ in a quantitative manner, because the small long-range oscillation of $g_{uv}(\vec{r})$ is amplified by the $4\pi|\vec{r}|^2$ factor, as seen in eq 2.5. Figure 1b shows that $\Delta V(\lambda) = 50 \pm 10$ Å^3 for $\lambda > 7$ Å. Variations in $g_{uv}(\vec{r})$ in the second and third hydration shells lead to fluctuations of $\Delta V(\lambda)$ by up to 20% as the cutoff is increased beyond $\lambda = 7$ Å.

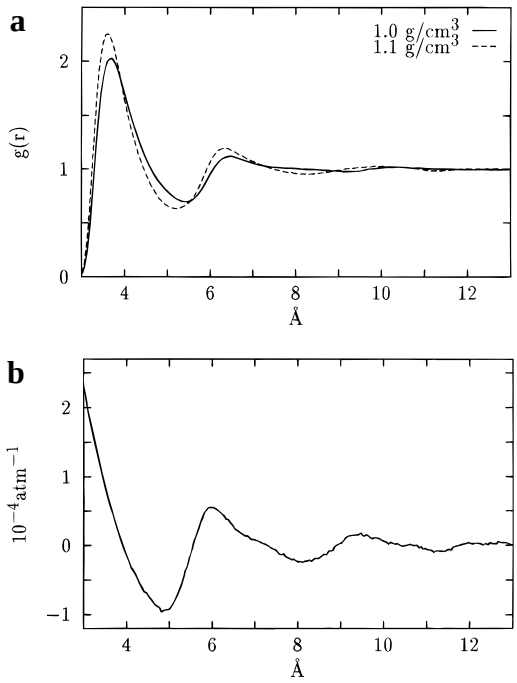

Figure 2. (a) Methane−water radial distribution functions at densities of 1.0 and 1.1 g/cm^3. (b) Difference between the local and bulk compressibilities.

The above estimate of ΔV based on the behavior of $\Delta V(\lambda)$ as a function of λ (Figure 1b) is in good agreement with the "exact" value calculated by the particle insertion method. ΔV is thus mostly determined by the solvent density within $|\vec{r}| < 7$ Å; i.e., the first two shells as determined by $g_{uv}(\vec{r})$ are responsible for ΔV. In the simplest hydration shell model, however, ΔV is interpreted in terms only of the solvent within the first peak of $g_{uv}(\vec{r})$. This interpretation is valid if the second shell does not make a net contribution to the excess volume. It is seen in Figure 1b that $\Delta V(\lambda)$ is close to the "exact" value at the interface between the first and second shells, i.e., at the first minimum in $g_{uv}(\vec{r})$ (at $\lambda = 5.5$ Å, $\Delta V(\lambda) = 60$ Å^3), and that consequently the second peak of $g_{uv}(\vec{r})$ does not make a net contribution to ΔV. Therefore, the negative hydration volume of methane in water can be attributed to the local accumulation of the solvent in the first hydration shell.

Finally, we note that the iceberg model of hydrophobic hydration of Frank and Evans[24] predicts very different volumetric behavior for the hydration shell than observed in the simulations (Figure 1). Taken literally, the contribution of an icelike shell to the excess volume would be expected to be positive rather than negative because the molar volume of ice is greater than that of liquid water. If the iceberg model helps to explain some features of hydrophobic hydration such as the enhanced structure or decreased entropy of water in the first shell, it is not a good model for the volumetric behavior (or the compressibility, see below), for which simple liquid-like packing effects provide a satisfactory basis for understanding the phenomena.

4.3. Excess Compressibility. In Figure 2a, we show the solute−solvent radial distribution functions $g_{uv}(\vec{r})$ at solvent densities of 1.0 and 1.1 g/cm^3. There is a large pressure effect on the solute−solvent radial distribution function. The amplitude of the oscillation in $g_{uv}(\vec{r})$ is larger at the higher density. The positions of the first maximum and minimum indicate that the packing is more efficient at the higher density. The density dependence of $g_{uv}(\vec{r})$ provides information about the local compressibility through eq 3.1. We show in Figure 2b the difference between the local and bulk compressibilities, $\partial \ln(g_{uv}(\vec{r}))/\partial P = \partial \ln(\varrho(\vec{r}))/\partial P - \partial \ln \varrho_0/\partial P$, as a function of the distance from the solute. It is seen, in agreement with the previous finding,[25] that the water at the first maximum in $g_{uv}(\vec{r})$ ($|\vec{r}| = 3.8$ Å) is more compressible than that in the bulk. Thus, the water at the first maximum contributes positively to the excess compressibility. The water in the first dense region (the first region in which $g_{uv}(\vec{r}) > 1$, i.e., 3.3 Å $< |\vec{r}| <$ 4.6 Å), however, does not show uniform behavior. As shown in Figure 2, the region centered on the first peak in the radial distribution function consists of two distinct regions in terms of the local compressibility; the region closer to the solute is more compressible than the bulk while the further region is less compressible. The behavior of the local compressibility in the first dense region observed in Figure 2 is therefore not as simple as that expected from the iceberg model for the hydration shell of a hydrophobic solute.[24] In the iceberg model, the solvent structure is "icelike" in the shell and it is therefore expected to be uniformly less compressible in the shell than in the bulk. The first sparse region (the first region in which $g_{uv}(\vec{r}) < 1$, i.e., 4.6 Å $< |\vec{r}| <$ 6.1 Å) also consists of more compressible and less compressible regions. In other words, the local density $g_{uv}(\vec{r})$ and the difference between the local and bulk compressibilities $\partial \ln(g_{uv}(\vec{r}))/\partial P$ are out of phase with each other. This is in contrast with the case of the binding energy treated in the previous paper,[1] for which the local density and the difference between the local and bulk binding energies are in phase with each other. The phase relationship between the local density and the local excess quantity plays an important role in determining the convergence property of the excess quantity as a function of the shell cutoff. We discuss this point in section 4.4.

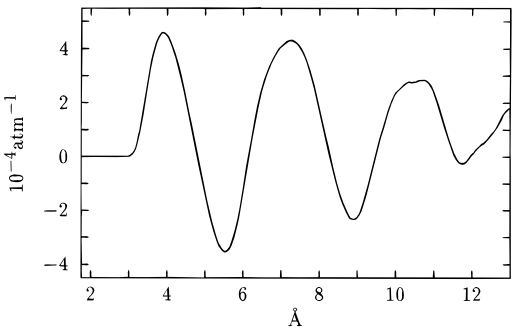

Figure 3. Excess compressibility as a function of the cutoff radius of the shell. The horizontal axis shows the cutoff radius of the shell, and the vertical axis shows the excess compressibility evaluated with this cutoff.

The excess compressibility $\Delta\kappa$ can be constructed from the local solvent compressibility through eq 2.12. In Figure 3, we show the excess compressibility of solvation $\Delta\kappa(\lambda)$ as a function of the hydration shell cutoff radius λ. The curve is so ill-behaved that even the sign of $\Delta\kappa$ is not clear. Thus, the convergence behavior of $\Delta\kappa(\lambda)$ given in Figure 3 shows that the hydration shell model is not successful, even qualitatively, for describing the excess compressibility.

4.4. Qualitative Validity of the Hydration Shell Model. In the previous paper[1] we examined the molecular basis for the hydration shell model for the excess energy. A corresponding analysis for the excess volume and compressibility has been performed in this paper. The hydration shell model is frequently used to provide a molecular interpretation of thermodynamic measurements. In this section, we discuss several conditions that must be satisfied for the hydration shell model to be useful, even qualitatively, as an interpretative tool. We emphasize the importance of the phase relationship between $g_{uv}(\vec{r})$ and the local excess quantities. As shown in the previous paper[1] and section

2, our hydration shell analysis of an excess thermodynamic quantity, ΔQ, begins with the expression

$$\Delta Q = \int \mathrm{d}\vec{r}\ \varrho(\vec{r})(q(\vec{r}) - q_0) \tag{4.1}$$

where $\varrho(\vec{r})$ is $\varrho_0 g_{uv}(\vec{r})$, $q(\vec{r})$ is the local quantity corresponding to the excess thermodynamic quantity ΔQ, and q_0 is its value for the neat liquid. The local quantity $q(\vec{r})$ is the binding energy for the excess energy,[1] the volume per solvent molecule $1/\varrho(\vec{r})$ for the excess volume (see eq 2.3), or the local compressibility $\partial \ln(\varrho(\vec{r}))/\partial P$ for the excess compressibility (see eq 2.11). Formally exact but practically intractable expressions for $q(\vec{r})$ are also available for the chemical potential and the excess entropy (see eqs A2.5 and A2.9 of the previous paper[1]). The difference $q(\vec{r}) - q_0$ can be considered to be the local excess contribution to the total excess quantity ΔQ. The hydration shell model is implemented by restricting the range of integration to a finite region proximate to the solute. As the system is rotationally invariant for the model employed in the previous paper[1] and this paper, we can write eq 4.1 using only the radial coordinate:

$$\Delta Q = \varrho_0 \int \mathrm{d}r\ g_{uv}(r)\Delta q(r) \tag{4.2}$$

where $r = |\vec{r}|$ and

$$\Delta q(r) = 4\pi|\vec{r}|^2(q(\vec{r}) - q_0) \tag{4.3}$$

If $\Delta q(r)$ decays fast with r, the introduction of a cutoff in eq 4.2 is a good approximation, and thus the hydration shell model is valid, not only qualitatively but also quantitatively. However, $\Delta q(r)$ does not decay rapidly for the binding energy, the volume per solvent molecule, or the local compressibility. It is actually an oscillatory function of r, so that compensation occurs between positive and negative contributions of $\Delta q(r)$ to ΔQ. For this case, the phase relationship between $g_{uv}(r)$ and $\Delta q(r)$ plays an important role in determining the sign of the excess quantity. We refer to the hydration shell model as qualitatively valid, when the sign of the excess quantity does not change as a function of the shell cutoff.

For the excess energy, $g_{uv}(r)$ and $\Delta q(r)$ have been found to be in phase with each other;[1] $\Delta q(r)$ is negative in each locally dense region (regions for which $g_{uv}(r) > 1$) and positive in each locally sparse region (regions for which $g_{uv}(r) < 1$). As the magnitude of $\Delta q(r)$ in each locally dense region is comparable to that in the subsequent locally sparse region and the width of the locally dense region is comparable to that of the subsequent locally sparse region, the negative contribution of $\Delta q(r)$ to ΔQ in the locally dense region is only partially canceled by the positive contribution of $\Delta q(r)$ in the subsequent locally sparse region. Therefore, each locally dense region and the subsequent locally sparse region together make a negative contribution to ΔQ as a whole, and the sign of ΔQ remains negative for any cutoff. This is clearly seen in Figure 3 of the previous paper.[1]

In the above discussion of the excess energy, the qualitative validity of the hydration shell model is due to the following conditions: (1) $\Delta q(r)$ and $g_{uv}(r)$ are in phase with each other, (2) the magnitude of $g_{uv}(r)\Delta q(r)$ in locally dense region is larger than that in the subsequent locally sparse region, and (3) the width of a locally dense region is comparable to that of the subsequent locally sparse region. For the excess volume, the first and second conditions are clearly satisified, but careful consideration is necessary for the third condition. In section 4.2, we suggested two reasonable choices for the exclusion radius σ for a soft solute−solvent interaction. Fulfillment of the third condition requires that the solvent-excluded region be defined to end at the first point at which $g_{uv}(\vec{r})$ reaches 1. In other words, when the excluded volume radius is chosen to be the sum of the van der Waals radii of the solute and solvent, then the hydration volume contribution to $\Delta V(\lambda)$ is negative for any choice of λ. Thus, the third condition gives the unique decomposition of the excess volume into the excluded volume (the first term of eq 2.6) and the hydration volume (the second term of eq 2.6). The width of each locally dense portion of the region occupied by solvent ($r > \sigma$) is comparable to that of the subsequent locally sparse portion (see Figure 1); the contributions of the adjacent regions to the excess volume partially cancel. In this sense, each locally dense region and the subsequent locally sparse region form a pair whose total contribution is negative. If however σ is chosen to be the van der Waals radius, the third condition is violated, and the sign of the hydration shell contribution to the excess volume oscillates as λ is varied. When the hydration effect on the excess volume is properly extracted as above, the local excess quantity satisfies the three conditions for the qualitative validity of the hydration shell model.

For the excess compressibility, $g_{uv}(r)$ and $\Delta q(r)$ are not in phase with each other (compare Figure 1a with Figure 2b). The cancellation between the positive and negative contributions of $\Delta q(r)$ to the integral eq 4.1 occurs also for this case, but it is not systematic from the perspective of the shell decomposition, as the above cases of the excess energy and volume. For example, as seen in Figure 2b, the width of the first positive region of $\Delta q(r)$ is only half that of the subsequent negative region. Therefore, even the sign of ΔQ cannot be clearly determined from knowledge of the behavior of $\Delta q(r)$ within the first peak of $g_{uv}(r)$. Conversely, the experimentally determined excess compressibility does not provide direct information about the response of the solvent within the first hydration shell to a pressure variation.

4.5. Concluding Remarks. In this paper, we have discussed the statistical mechanical foundation of the hydration shell model of the excess volume and compressibility and its application to the hydrophobic solute methane in water. Although the thermodynamic analysis of methane in water provides a prototype system useful for understanding solution phenomena, a discussion of the hydration shell model as applied to larger molecules is more relevant from the perspective of current problems in solution biochemistry. In empirical applications of the hydration shell model (e.g. see ref 26), the additivity of the contributions from various functional groups is assumed. In subsequent work, we will analyze this assumption by determining the extent to which the local excess quantity for a functional group is modified by the presence of the neighboring functional groups and relate the extent of additivity to the validity of the commonly used surface area arguments concerning excess thermodynamic quantities.[26] Finally, while our molecular approach for solvation employs realistic molecular interaction potentials, scaled particle theory (SPT) provides a less computationally demanding treatment of solvation phenomena.[6,27−29] It would be interesting to develop connections between SPT-type models and hydration shell models.

Acknowledgment. We thank Dr. Lynne Reed Murphy and Dr. Vilia A. Payne for valuable discussions. This work has been supported by a grant from the National Institutes of Health (GM-52210) and by the allocation of computer resources by the NSF MetaCenter Program.

Appendix

In this Appendix, we show the relation of $\Delta\kappa$ defined as in eq 2.10 to the observed change in the compressibility upon

solute insertion at constant pressure. Let N_s be the number of solute molecules in the solution and $V(N_s)$ be the solution volume at that number of solute molecules. With the definition of the partial molar volume of the solute, we obtain

$$V(N_s) = V_0 + N_s\bar{V}_s + O(N_s^2) \tag{A.1}$$

where V_0 is the volume of the pure solvent and $\bar{V}_s$ is the partial molar volume of the solute at infinite dilution. The relationship between $\bar{V}_s$ and the excess volume ΔV treated in this paper is given by eq 2.2:

$$\bar{V}_s = \Delta V + kT\kappa_0 \tag{A.2}$$

where k is the Boltzmann constant, T is the temperature, and κ_0 is the isothermal compressibility of the pure solvent. Through the definition of the excess compressibility $\Delta\kappa$ given by eq 2.10, the differentiation of eq A.2 with respect to pressure leads to

$$\frac{\partial\bar{V}_s}{\partial P} = kT\frac{\partial\kappa_0}{\partial P} - \frac{\Delta\kappa}{\varrho_0} \tag{A.3}$$

where P is the pressure of the system, which is held constant upon solute insertion.

The experimentally observed compressibility of the solution, $\kappa(N_s)$, is by definition the rate of change in the solution volume with pressure variation:

$$\kappa(N_s) = -\frac{1}{V(N_s)}\frac{\partial V(N_s)}{\partial P} \tag{A.4}$$

Substituting eqs A.1, A.2, and A.3 into eq A.4, we obtain

$$\begin{aligned}\kappa(N_s) &= -\frac{1}{V_0}\left(\frac{\partial V_0}{\partial P} + N_s\frac{\partial\bar{V}_s}{\partial P} - \bar{V}_s\frac{N_s}{V_0}\frac{\partial V_0}{\partial P}\right) + O(N_s^2)\\ &= \kappa_0 + \left[\frac{\Delta\kappa}{\varrho_0} - \kappa_0\Delta V - kT\kappa_0\left(\kappa_0 + \frac{\partial \ln \kappa_0}{\partial P}\right)\right]\varrho_s + O(\varrho_s^2)\end{aligned} \tag{A.5}$$

where ϱ_s is the solute concentration in the solution. Each term in the square brackets on the right-hand side of the above equation can be evaluated from the numerical results presented in section 4.1. The first, second, and third terms are calculated to be 6.0×10^{-5}, -1.8×10^{-6}, and 4.0×10^{-7} (atm^{-1})(L/mol), respectively. Therefore, the factor $\Delta\kappa/\varrho_0$ determines about 97% of the first-order effect of the solute on the solution compressibility.

References and Notes

(1) Matubayasi, N.; Reed, L. H.; Levy, R. M. *J. Phys. Chem.* **1994**, *98*, 10640.
(2) Kirkwood, J. G.; Buff, F. P. *J. Chem. Phys.* **1951**, *19*, 774.
(3) Pratt, L. R.; Pohorille, A. *Proc. EBSA Workshop on Water−Biomolecule Interactions* **1992**, *43*, 261.
(4) Paulaitis, M. E.; Ashbaugh, H. S.; Garde, S. *Biophys. Chem.* **1994**, *51*, 349.
(5) Ben-Naim, A. *Solvation Thermodynamics*; Plenum, New York, 1987.
(6) Yoshimura, Y.; Nakahara, M. *J. Chem. Phys.* **1984**, *81*, 4080.
(7) Evans, M. G.; Polanyi, M. *Trans. Faraday Soc.* **1935**, *31*, 875.
(8) Yoshimura, Y.; Osugi, J.; Nakahara, M. *J. Am. Chem. Soc.* **1983**, *105*, 5414.
(9) Ladanyi, B. M.; Hynes, J. T. *J. Am. Chem. Soc.* **1986**, *108*, 585.
(10) Murphy, L. R.; Matubayasi, N.; Levy, R. M. Manuscript in preparation.
(11) Allen, M. P.; Tildesley, D. J. *Computer Simulation of Liquids*; Oxford University Press, Oxford, 1987.
(12) Jorgensen, W. L.; Chandrasekhar, J.; Madura, J. D.; Impey, R. W.; Klein, M. L. *J. Chem. Phys.* **1983**, *79*, 926.
(13) Smith, D. E.; Haymet, A. D. J. *J. Chem. Phys.* **1993**, *98*, 6445.
(14) Owicki, J. C.; Scheraga, H. A. *Chem. Phys. Lett.* **1977**, *47*, 600.
(15) Guillot, B.; Guissani, Y.; Bratos, S. *J. Chem. Phys.* **1991**, *95*, 3643.
(16) Gibson, R. E.; Loeffler, O. H. *J. Am. Chem. Soc.* **1941**, *63*, 898.
(17) Sawamura, S.; Kitamura, K.; Taniguchi, Y. *J. Phys. Chem.* **1989**, *93*, 4931.
(18) Chalikian, T. V.; Sarvazyan, A. P.; Breslauer, K. J. *Biophys. Chem.* **1994**, *51*, 89.
(19) The experimental value reported in ref 18 is not the excess isothermal compressibility but the excess adiabatic compressibility. The excess isothermal compressibility can be calculated from the excess adiabatic compressibility, the excess expansion coefficient, and the excess heat capacity through a thermodynamic identity and is found to still be negative.
(20) We also calculated $\Delta\kappa$ at a temperature of 25 °C using the particle insertion method and found that $\Delta\kappa$ is negative at 25 °C.[21] Thus, the sign of $\Delta\kappa$ at 25 °C calculated from the simulations is coincident with the observed sign of the excess compressibility per methylene group.[17,18] But $\Delta\kappa$ depends sensitively on the temperature; in the simulations, the sign changes from positive to negative with the temperature variation from 10 to 25 °C. This temperature dependence is not consistent with the experimental observation.[17,18] The temperature dependence of $\Delta\kappa$ is a third-order derivative of the chemical potential. A better framework for understanding such a higher order property is clearly needed.
(21) Matubayasi, N. Ph.D. Thesis, Rutgers University, 1995.
(22) Brandts, J. F.; Oliveira, R. J.; Westort, C. *Biochemistry* **1970**, *9*, 1038.
(23) Hawley, S. A. *Biochemistry* **1971**, *10*, 2436.
(24) Frank, H. S.; Evans, M. W. *J. Chem. Phys.* **1945**, *13*, 507.
(25) Kitchen, D. B.; Reed, L. H.; Levy, R. M. *Biochemistry* **1992**, *31*, 10083.
(26) Ooi, T.; Oobatake, M.; Némethy, G.; Scheraga, H. A. *Proc. Natl. Acad. Sci.* **1987**, *84*, 3086.
(27) Pierotti, R. A. *J. Phys. Chem.* **1965**, *69*, 281.
(28) Stillinger, F. H. *J. Solution Chem.* **1973**, *2*, 141.
(29) Ben-Amotz, D. *J. Phys. Chem.* **1993**, *97*, 2314.

JP951618B